Molecular Biology of the Cell
Vol. 18, 1744–1755, May 2007

The MAGUK Protein MPP7 Binds to the Polarity Protein hDlg1 and Facilitates Epithelial Tight Junction Formation[D]

Volker M. Stucke,* Evy Timmerman,† Joel Vandekerckhove,† Kris Gevaert,† and Alan Hall*‡

*Medical Research Council Laboratory for Molecular Cell Biology, Cancer Research UK Oncogene and Signal Transduction Group, University College London, London WC1E 6BT, England; and †Department of Medical Protein Research, Flanders Interuniversity Institute for Biotechnology and Department of Biochemistry, Ghent University, B-9000 Ghent, Belgium

Submitted November 1, 2006; Revised January 16, 2007; Accepted February 15, 2007
Monitoring Editor: Ben Margolis

Three groups of evolutionarily conserved proteins have been implicated in the establishment of epithelial cell polarity: the apically-localized proteins of the Par (Par3-Par6-aPKC-Cdc42) and Crumbs groups (Crb3-PALS1-PATJ) and the basolaterally localized proteins of the Dlg group (Dlg1-Scribble-Lgl). During epithelial morphogenesis, these proteins participate in a complex network of interdependent interactions that define the position and functional organization of adherens junctions and tight junctions. However, the biochemical pathways through which they control polarity are poorly understood. In this study, we identify an interaction between endogenous hDlg1 and MPP7, a previously uncharacterized MAGUK-p55 subfamily member. We find that MPP7 targets to the lateral surface of epithelial cells via its L27N domain, through an interaction with hDlg1. Loss of either hDlg1 or MPP7 from epithelial Caco-2 cells results in a significant defect in the assembly and maintenance of functional tight junctions. We conclude that the formation of a complex between hDlg1 and MPP7 promotes epithelial cell polarity and tight junction formation.

INTRODUCTION

The establishment of cell polarity and the formation of multicellular tissues and organs are fundamentally important in the development of higher eukaryotes (Schock and Perrimon, 2002). In epithelial sheets, cells are polarized with apical and basolateral membrane domains separated by tight junctions, specialized sites of intimate cell–cell contact that act as a barrier to the free diffusion of lipid and proteins (Yeaman *et al.*, 1999). Numerous proteins and signal transduction pathways have been implicated in the establishment of cell polarity, but genetic analyses in *Drosophila* and *Caenorhabditis elegans* have identified three groups of highly conserved proteins that play a critical role in this process (Macara, 2004). These are: 1) Par3, Par6, and aPKC (Joberty *et al.*, 2000; Lin *et al.*, 2000; Wodarz *et al.*, 2000; Petronczki and Knoblich, 2001; Tepass *et al.*, 2001); 2) Crb3, PALS1 (MPP5), and PATJ, which are both located predominantly apically (Bachmann *et al.*, 2001; Hong *et al.*, 2001; Tepass *et al.*, 2001; Medina *et al.*, 2002); and 3) Dlg1, Scribble, and Lgl, located mostly on the basolateral surfaces (Bilder *et al.*, 2000; Bilder and Perrimon, 2000; Bossinger *et al.*, 2001; Tepass *et al.*, 2001). With the exception of aPKC, members of these three groups of proteins lack catalytic activity. Instead they contain multiple protein–protein interaction domains, in particular PDZ, SH3, and guanylate kinase domains often referred to as membrane-associated guanylate kinase or MAGUK proteins (Funke *et al.*, 2005), indicating a complex network of protein interactions controlling cell polarity.

Par3, Par6, and the activity of aPKC regulate the assembly of functional tight junctions in mammalian cells (Yamanaka *et al.*, 2001; Suzuki *et al.*, 2002). These proteins physically interact with each other. Par3, which contains three PDZ domains, for example, binds to the PDZ domain of Par6 (Joberty *et al.*, 2000; Lin *et al.*, 2000) and is able to associate with cell adhesion molecules such as Jam1 (Ebnet *et al.*, 2001) or nectin (Takekuni *et al.*, 2003). Both Par3 and Par6 can bind to aPKC, whereas the GTP-bound form of Cdc42 interacts with Par6 via a Cdc42/Rac-interactive binding (CRIB)-like motif to regulate aPKC activity (Izumi *et al.*, 1998; Tabuse *et al.*, 1998; Joberty *et al.*, 2000; Lin *et al.*, 2000; Qiu *et al.*, 2000; Suzuki *et al.*, 2001). The transmembrane protein Crb3 and its binding partners PALS1 (MPP5) and PATJ are also required for tight junction integrity (Roh *et al.*, 2003; Straight *et al.*, 2004; Shin *et al.*, 2005). Crb3 binds through a carboxy-terminal motif to the PDZ domain of PALS1 (MPP5; Makarova *et al.*, 2003; Roh *et al.*, 2003) and in turn, PALS1 binds to PATJ through L27 domain interactions (Lemmers *et al.*, 2002; Roh *et al.*, 2002b). The multi-PDZ domain protein PATJ is able to associate with tight junction–associated proteins such as ZO-3 and claudin-1 (Roh *et al.*, 2002a), providing a physical link to tight junctions. The third group of polarity proteins, the tumor suppressor proteins Dlg1, Scribble and Lgl have not been shown to physically associate with each other. However, mutations in any one of these genes disrupt api-

This article was published online ahead of print in *MBC in Press* (http://www.molbiolcell.org/cgi/doi/10.1091/mbc.E06–11–0980) on March 1, 2007.

[D] The online version of this article contains supplemental material at *MBC Online* (http://www.molbiolcell.org).

‡ Present address: Memorial Sloan-Kettering Cancer Center, 1275 York Avenue, Box 572, New York, NY 10021.

Address correspondence to: Alan Hall (halla@mskcc.org).

Abbreviations used: PDZ, PSD-95, ZO-1, and Discs-large; MPP, membrane-palmitoylated protein.

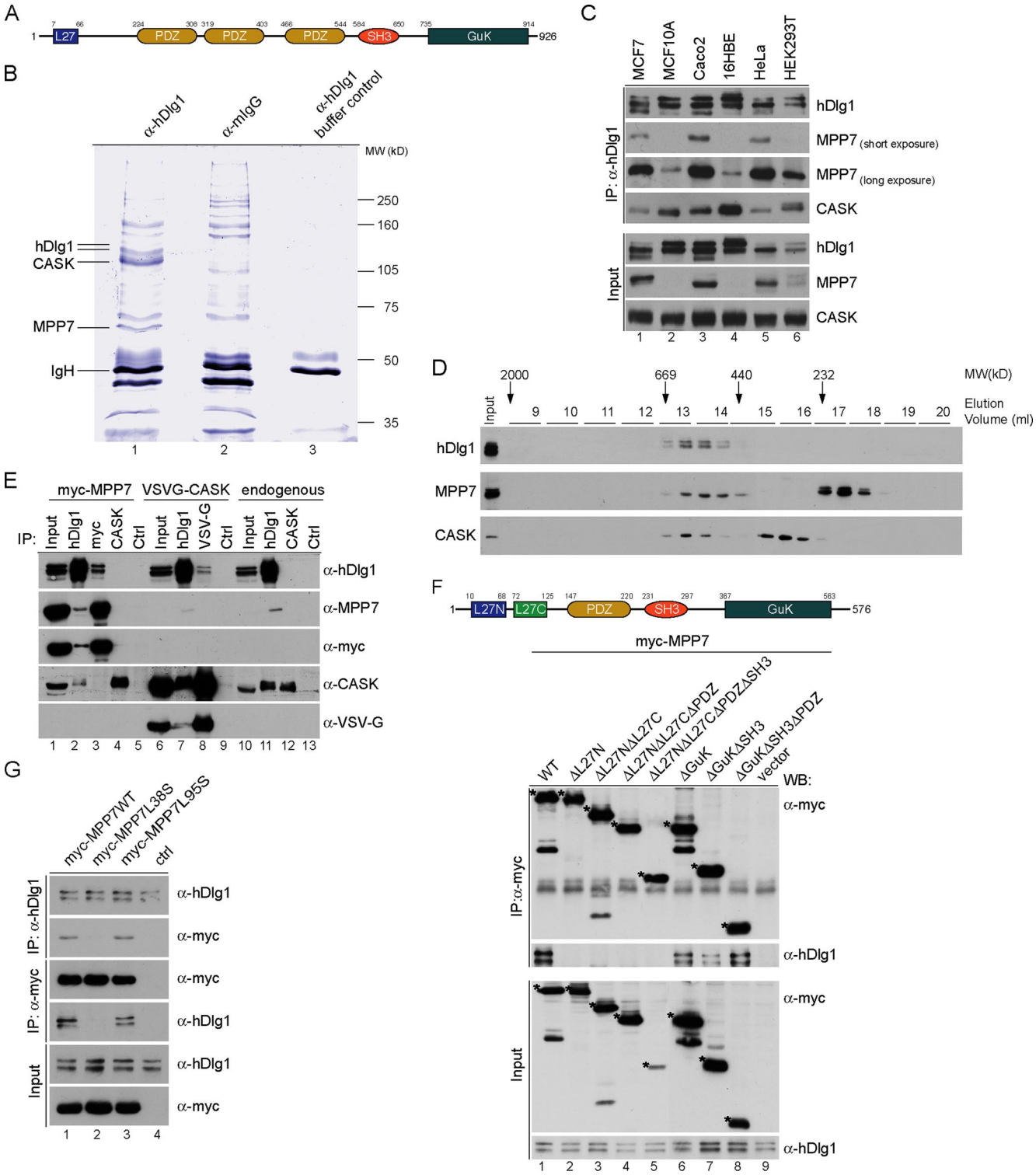

Figure 1. Identification and characterization of CASK and MPP7 as binding partners for hDlg1. (A) Schematic representation of the hDlg1 protein (amino acid numbers are given above) as indicated. (B) Colloidal blue-stained gel of an hDlg1 immunoprecipitate from MCF7 cell extracts (lane 1). A control immunoprecipitation was performed with mouse monoclonal α-myc antibody (mIgG; lane 2) or with anti-hDlg1 mAb alone without incubation in cell extracts (lane 3). Note the precipitated ~140-kDa hDlg1 isoforms, the ~110-kDa CASK protein, and the 65-kDa MPP7 protein identified by tryptic peptide fingerprinting. Molecular weight (MW) markers are indicated on the right. (C) Cell lysates of different epithelial cell lines were immunoprecipitated with hDlg1-antibodies. Proteins were detected by immunoblotting with antibodies against hDlg1, MPP7, and CASK. Note the very low MPP7 expression in MCF10A mammary breast epithelial cells and 16HBE lung epithelial cells. (D) Lysates made from polarized MCF7 cell monolayers were fractionated on a Superose-6 gel filtration column and fractions analyzed by Western blots for hDlg1, MPP7, and CASK. The elution volume and the native molecular mass standards are indicated. (E) Immunoprecipitations were performed from extracts of HEK 293T cells expressing myc-MPP7 (lanes 1–5), VSVG-CASK (lanes 6–9) or untransfected cells (lanes 10–13) with antibodies as indicated. Expression of the transfected constructs was monitored by Western blotting with anti-myc

cal-basal polarity in epithelial cells in *Drosophila melanogaster* (Woods *et al.*, 1996; Bilder *et al.*, 2000; Tanentzapf and Tepass, 2003; Bilder, 2004). shRNA-mediated depletion of hScrib leads to a delay in tight junction formation in MDCKII epithelial cells (Qin *et al.*, 2005).

A key question is how the proteins in these three groups communicate with each other to promote epithelial polarity and tight junction formation. Based on genetic studies in *D. melanogaster*, there appears to be a complex interplay between these groups, which includes positive and negative feedback loops (Bilder *et al.*, 2003; Tanentzapf and Tepass, 2003). The specification of the apical domain by Par proteins is thought to be an early event, which then leads to recruitment of the Crb group to this region. The Dlg group of proteins is recruited basolaterally, and their localization is restricted by antagonistic activities of the Crb group. However, it remains a major challenge to define the biochemical steps that generate a polarized epithelial cell monolayer.

Using a biochemical approach, we have identified a previously uncharacterized member of the MAGUK family, MPP7, as a novel protein that interacts with hDlg1. Using RNAi-mediated depletion in Caco2 cells, we show that both proteins are involved in the functional regulation of tight junction formation.

MATERIALS AND METHODS

Materials and Molecular Biology

All chemicals were obtained from Sigma-Aldrich (St. Louis, MO) or Merck (Rahway, NJ) unless otherwise specified. Cell culture media and sera were obtained from Invitrogen (Carlsbad, CA) and Mycoplex (A15–043) (PAA, Pasching, Austria), respectively. Cytochalasin D was from Sigma. DNA primers were synthesized by Sigma-Genosys, and synthetic RNA duplexes by Dharmacon Research (Boulder, CO). Restriction enzymes were purchased from New England Biolabs (Beverly, MA), and reagents for the purification of DNA from QIAGEN (Chatsworth, CA). Full-length human cDNAs for MPP7 (IRATp970B0732D6), MPP5 (DKFZp451E015Q2), and MPP3 (IRAKp961D21119Q2) were obtained from the Deutsches Ressourcenzentrum fuer Genomforschung (RZPD; GmbH, Berlin, Germany). Full-length human Crb3 was amplified from a Caco-2 cDNA library using Pfu polymerase (Stratagene, La Jolla, CA) and oligonucleotides 5′-GCCACCGGATCCATGGCGAACCCCGGGCTGGGGCTG-3′ and 5′-CCGAATTCCTCAGATGAGCCGCTCTTCCGGCGG-3′. VSVG-tagged CASK constructs were obtained by Z. Walther (Yale University, New Haven, CT). Point mutants were constructed using the QuikChange mutagenesis protocol (Stratagene). All constructs were confirmed by DNA sequencing (MWG-Biotech, Ebersberg, Germany). Mammalian expression constructs were made in pRK5-myc and pRK5-FLAG.

Cell Culture, Transfection, and RNA Interference

MCF7, HEK 293T, HeLa, and Caco-2 cells were cultured at 37°C in a 5% CO_2 atmosphere in Dulbecco's modified Eagle's medium (Invitrogen-BRL), supplemented with 10% fetal calf serum and penicillin-streptomycin (100 IU/ml and 100 mg/ml, respectively). MCF10A cells were cultured at 37°C in a 5% CO_2 and maintained in DMEM/F12 (Invitrogen-BRL) supplemented with 5% donor horse serum, 20 ng ml^{-1} EGF, 10 μg ml^{-1} insulin, 1 ng ml^{-1} cholera toxin, 100 μg ml^{-1} hydrocortisone, 50 U ml^{-1} penicillin, and 50 μg ml^{-1} streptomycin. MCF7 and MCF10A were transiently transfected using Lipofectamine 2000 (Invitrogen) and HEK 293T were transfected using GeneJuice (Novagen, Madison, WI). For small interfering RNA (siRNA) experiments, the following target sequences were used: MPP7-A (5′-GGAUACCAGUGGAGGAUAA-3′, nt 569-587); MPP7-B (5′-UGAAUGAACUGAAACGAAA-3′, nt 1142-1160); hDlg1-A (5′-CCACAAGUAUGUAUAUGAA-3′, nt 1214-1232); hDlg1-B (5′-AGAAGUUACUCAUGAAGAA-3′, nt 1140-1158); CASK-A (5′-GTAGCCAGCCATTATATGA-3′, nt 349-367); and CASK-B (5′-GGCAACAAUUUGCUGUAAA-3′, nt 104-122).

Oligonucleotides were annealed and transfected using oligofectamine (Invitrogen) as described by the manufacturer. As a control, a scrambled sequence was chosen.

Retrovirus Construction and Infection

The retroviral vector pSUPER.retro was purchased from OligoEngine (Seattle, WA). The following oligonucleotides were designed: MPP7-A (5′-GATCCCCggataccagtggaggataaTTCAAGAGAttatcctccactggtatccTTTTTA-3′, nt 569-587), MPP7-B (5′-GATCCCCggatgttcagcctcatacaTTCAAGAGA tgtatgaggctgaacttgaacatccTTTTTA-3′, nt 1392-1410), hDlg1-A (5′-GATCCCCcagaagctgttcttccctcTTCAAGAGAgagggaagaacagcttctgTTTTTA-3′, nt 488-506), hDlg1-B (5′-GATCCCCgcgttgaaagaagcagggtTTCAAGAGA accctgcttctttcaacgcTTTTTA-3′, nt 883-901). Complementary oligonucleotides were annealed and cloned into the unique BglII-HindIII sites downstream of the H1 RNA promoter, and inserts were confirmed by sequencing. Amphotropic retroviruses were produced by transfection of DNA constructs into the retroviral packaging cell line 293-GPG using Lipofectamine (Invitrogen). The medium was changed 24 h after transfection, and 72 h after transfection viral supernatant was collected, filtered through a 0.45-μm membrane, and stored at −80°C. Caco-2 cells (5×10^5 cells/10-cm plate) were infected with viral supernatants supplemented with polybrene (8 μg/ml). Forty-eight hours after infection, Caco-2 cells were grown in selection media containing 6 μg/ml puromycin to select for cells stably expressing the retroviral vector. Puromycin-resistant Caco-2 cells were maintained in media containing 6 μg/ml puromycin.

Transepithelial Electrical Resistance Measurements and Calcium Switch

Caco-2 cells were grown to confluence on permeable, collagen-coated Transwell filters (Becton Dickinson, Lincoln Park, NJ; Cat. no. 354804) for 5 d, washed extensively with PBS, and then incubated in low-calcium medium overnight (16 h) to dissociate cell–cell contacts. The low-calcium medium was replaced the next day with normal growth medium (1.8 mM Ca^{2+}), and transepithelial electrical resistance (TER) measurements were determined with a Millicell-ERS volt-ohm meter (Millipore, Billerica, MA), according to manufacturer's instructions, at various times afterward. Background resistance was determined using cell-free filters. Samples for each time point were measured in triplicate in a total of three independent experiments.

Antibody Reagents

Primary Antibodies were obtained as follows: mouse monoclonals to myc (Clone 9E10; Cancer Research UK, London, United Kingdom), VSV-G (clone PSD5; Cancer Research UK), FLAG (clone M2; Sigma-Aldrich), hDlg1 (clone 2D11; Santa Cruz Biotechnology, Santa Cruz, CA), E-cadherin (clone 4A2C7; Zymed, South San Francisco, CA), occludin (clone OC-3F10; Zymed), β-catenin (clone 14; BD Transduction Laboratories, Lexington, CA), CASK (clone K56A; Chemicon, Temecula, CA), α-tubulin (clone DM1a; Sigma-Aldrich), rabbit polyclonal antibodies to occludin (71-1500; Zymed), ZO-1 (61-7300; Zymed), CASK (71-5000; Zymed), FLAG (ab21536-100; Abcam, Cambridge, United Kingdom) and myc (MYC13-A; Alpha Diagnostics International, San Antonio, TX). A rabbit antibody against human MPP7 was raised against the peptide EVTPYRRQTNEKYR (amino acids 356-369) coupled to keyhole limpet hemocyanin. Antibodies were affinity-purified on the antigenic peptide covalently bound to SulfoLink Coupling Gel according to the manufacturer's instructions (Pierce Biotechnology, PERBIO Science GmbH, Bonn, Germany). The specificity of the MPP7 antibody is shown in the Supplementary Figure S1A. The antibody does not show cross-reactivity to other MAGUK proteins in total cell extracts and does not recognize ectopically expressed myc-MPP3 (the closest homolog of MPP7 of the p55-MAGUK subfamily).

Immunofluorescence Microscopy

Immunofluorescence microscopy was performed on MCF7 cells or Caco-2 cells grown on coverslips. Cells were fixed with 3% [wt/vol] paraformaldehyde for 15 min at RT, quenched for 10 min with 50 mM ammonium chloride, and permeabilized with 0.1% [vol/vol] Triton X-100 for 5 min. Alternatively, cells were fixed in −20°C methanol for 6 min. Blocking for 30 min at RT and sequential incubation of primary and secondary antibodies for 1 h at RT were done in PBS containing 3% BSA. Primary antibodies used in this study were as follows: rabbit polyclonal, affinity-purified pα-MPP7 (10 μg/ml), pα-α-catenin (1:200), pα-occludin (1:200), and pα-FLAG (1:500) and mouse monoclonal mα-hDlg1 (1:100), mα-CASK (1:200), mα-E-cadherin (1:200), mα-occludin (1:200), and mα-myc (1:100). Secondary antibodies conjugated to either Alexa 488, Alexa 568, or Texas Red were used to visualize antibody staining

Figure 1 (cont). or anti-VSVG antibodies (Input). (F) Immunoprecipitations (IPs) were performed using myc antibodies from HEK 293T cells transfected with MPP7 constructs as indicated. Samples of the lysates and myc IPs were analyzed by Western blotting for hDlg1 and the myc epitope. A schematic representation of the human MPP7 protein (amino acid numbers are given above) is shown on the top and exogenously expressed MPP7 proteins are marked by asterisks (*). (G) Myc-tagged MPP7WT, MPP7L38S, and MPP7L95S were transfected into HEK 293T cells. Lysates from each condition were split and immunoprecipitated with either hDlg1 (panels 1 and 2) or myc (panels 3 and 4) antibodies and then immunoblotted with hDlg1 or myc antibodies, as indicated. All experiments shown in Figure 1 are representatives of three independent experiments.

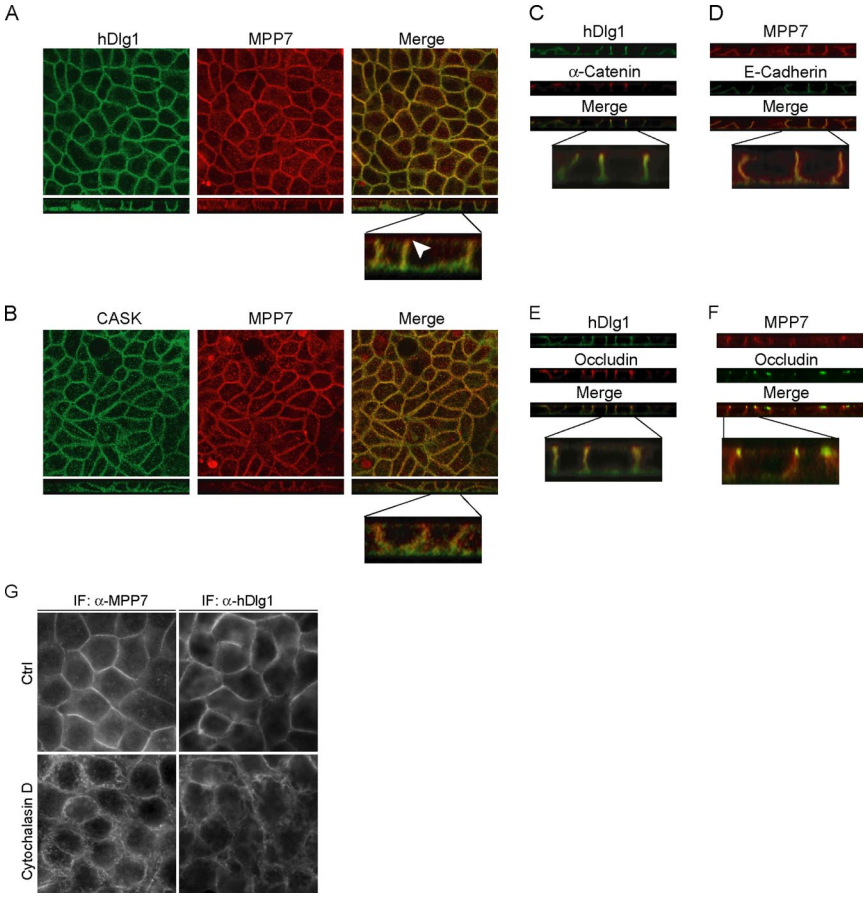

Figure 2. MPP7 and hDlg1 colocalize at the lateral surface in Caco-2 cells. (A and B) Confocal microscopic *X-Y* sections near the cell junctions of Caco-2 cells grown to confluence for 14 d, fixed, and stained with antibodies to (A) hDlg1 (green) and MPP7 (red) and (B) CASK (green) and MPP7 (red). The right panels are a merge of the left and middle images. Below each panel is the corresponding *Z*-section showing the apical-basolateral localization of the proteins (apical at the top, basolateral at the bottom). Arrowhead indicates the more apical localization of MPP7 compared with hDlg1. (C–F) *Z*-sections of Caco-2 cells grown as described in A. Cells were fixed and stained with antibodies to adherens junction markers in C) for α-Catenin (red) and hDlg1 (green) and (D) for E-Cadherin (green) and MPP7 (red). Cells were fixed and stained with antibodies to tight junction markers in E for Occludin (red) and hDlg1 (green) and (F) Occludin (green) and MPP7 (red). Merged images are shown in the bottom panels. All images were acquired using the same settings on the confocal microscope. (G) MCF7 cells were treated with either 2 μM cytochalasin D or DMSO (Ctrl) for 1 h before fixation and stained with antibodies for MPP7 and hDlg1 as indicated. Under these conditions, hDlg1 and MPP7 lose their association with the plasma membrane and relocalize to the cytoplasm. All experiments shown in Figure 2 are representatives of three independent experiments.

(1:1000, Molecular Probes, Eugene, OR). DNA was stained with Hoechst 33342 (1:20.000, Molecular Probes). Images were collected with a Zeiss Axioplan microscope using a 63× Plan Apochromat oil immersion objective (NA 1.4; Zeiss, Jena, Germany), standard filter sets and an ORCA-ER (Hamamatsu, Bridgewater, NJ) camera driven by Openlab software (Improvision, Lexington, MA). Confocal images were obtained with a MRC1024 (Bio-Rad, Richmond, CA) confocal OptiphotII (Nikon, Melville, NY) microscope using a 60× planapochromatic objective (NA 1.4). Images were cropped in Adobe Photoshop 7.0, sized, and placed in figures using Adobe Illustrator 10.0 (Adobe Systems, San Jose, CA).

Cell Lysates, Immune Precipitations, and Immunoblotting

MCF7, MCF10A, and HEK 293T cells were washed twice in ice-cold PBS, 1 mM phenylmethylsulfonyl fluoride (PMSF) and resuspended in lysis buffer (25 mM HEPES, pH 7.4, 150 mM NaCl, 1 mM $MgCl_2$, 1 mM EGTA, 0.5% [vol/vol] Triton X-100, 5 mM NaF, 20 mM β-glycerophosphate, 100 μM Na_3VO_4, 1 mM PMSF, and protease inhibitor cocktail tablet [Roche]). Cell debris was pelleted by centrifugation at 14,000 rpm for 15 min at 4°C. Protein concentrations were determined using the Dc protein assay (Bio-Rad). For immune precipitations, equal amounts of cell extracts were precleared using protein G-Sepharose for 1 h at 4°C. They were then incubated with 1 μg of affinity-purified antibody for 2 h before 20 μl protein G- or A-Sepharose beads were added for 60 min. All incubations were performed on a rotating wheel. Immune complexes were spun down, washed three times with lysis-buffer containing 250 mM NaCl, and then boiled in SDS-PAGE sample buffer. For immunoblotting, proteins were resolved by SDS-PAGE and electrophoretically transferred to nitrocellulose membranes (Schleicher & Schuell, Keene, NH). Membranes were stained with Ponceau S, blocked in 5% nonfat dry milk in PBS for 1 h at RT, and incubated overnight at 4°C with either rabbit polyclonal, affinity-purified primary MPP7 antibody (2 μg/ml), pα-ZO-1 (1:1000), pα-occludin (1:4000) or mouse monoclonal α-hDlg1 antibody (1:500), mα-CASK (1:1000), mα-tubulin (1:4000), mα-myc (1:500), mα-FLAG (1:1000), mα-E-cadherin, mα-β-catenin, and mα-VSV-G (all 1:1000). The membranes were washed with 0.05% Triton X-100/PBS, followed by incubation with horseradish peroxidase (HRP)-conjugated secondary antibody (Pierce) in 5% nonfat dry milk in PBS for 1 h at room temperature, and then washed with 0.05% Triton X-100/PBS. Bound HRP-conjugated antibodies were visualized with the enhanced chemiluminescence (ECL) detection system (GE Healthcare, Buckingham, United Kingdom).

Purification of the hDlg1 Complex, Mass Spectrometry, and Gel Filtration Chromatography

For the purification of the hDlg1 complex, a total of 50 plates (150 mm) of MCF7 cells were grown to confluency. After washing the cells twice in ice-cold PBS containing 1 mM PMSF, they were resuspended in lysis buffer (25 mM HEPES, pH 7.4, 150 mM NaCl, 1 mM $MgCl_2$, 1 mM EGTA, 0.5% [vol/vol] Triton X-100, 5 mM NaF, 20 mM β-glycerophosphate, 100 μM Na_3VO_4, 1 mM PMSF and protease inhibitor cocktail tablet [Roche]). Cell debris was pelleted by centrifugation at 14,000 rpm for 15 min at 4°C. The supernatant was then centrifuged at 40,000 rpm for 1 h at 4°C, and the remaining supernatant was precleared using protein G-Sepharose for 1 h at 4°C. For immune precipitations, equal amounts of MCF7 cell extracts were incubated with 8 μg mα-hDlg1 antibody and control IgG1 for 14 h at 4°C, followed by the addition of protein G-Sepharose, rotating continuously. Immune complexes were washed four times with lysis buffer, 50 μl of reducing sample buffer was added, and then beads were heated at 95°C for 5 min, followed by the analysis on 7.5% minigels.

Coomassie-stained proteins of interest were excised and in-gel digested with trypsin as described (Gevaert and Vandekerckhove, 2005). The generated peptide mixture was dried, redissolved in 20 μl of 0.1% formic acid in 2/98 (vol/vol) acetonitrile/water, and 10 μl was applied for nano-LC-MS/MS analysis using an Ultimate (Dionex, Amsterdam, The Netherlands) HPLC system in-line connected to an Esquire HCT ion trap (Bruker Daltonics, Bremen, Germany). Peptides were first trapped on a trapping column (PepMap C18 column, 0.3 mm ID × 5 mm, Dionex) and after back-flushing, they were loaded on a 75 μm ID × 150-mm reverse-phase column (PepMap C18, Dionex). The peptides were eluted with a linear solvent gradient over 50 min ending in 0.1% of formic acid in acetonitrile/water (7/3, vol/vol). Using data-dependent acquisition, only multiple charged ions with intensities above a threshold of 100,000 were selected for further fragmentation. For MS/MS analysis, a MS/MS fragmentation amplitude of 0.7 V and a scan time of 40 ms were used. The fragmentation spectra were converted to Mascot generic files (mgf) using the Automation Engine software (version 3.2, Bruker) and searched using MASCOT (http://www.matrixscience.com) against the human IPI database (http://www.ebi.ac.uk/IPI/IPIhelp.html). Only spectra that exceeded Mascot's threshold score for identify (set at the 95% confidence level) were reported for further manual validation.

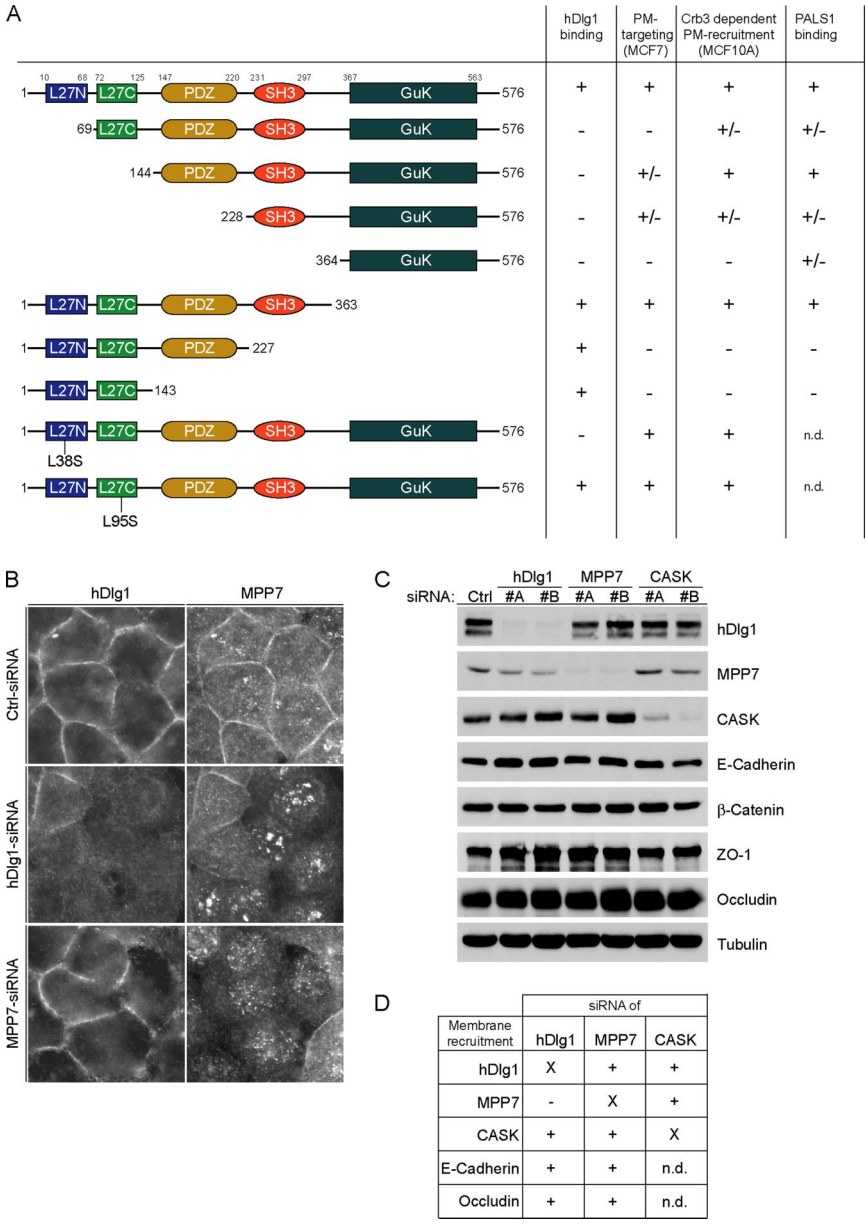

Figure 3. hDlg1 is required for plasma membrane localization of MPP7. (A) Schematic representation of the different myc-MPP7 constructs used to examine their ability to bind to hDlg1 in HEK 293T cells (first column), to target to the plasma membrane in MCF7 cells (second column), to be recruited to the plasma membrane in a Crb3-dependent manner in MCF10A cells (third column), and to bind to PALS1/MPP5 (fourth column). Numbers refer to the amino acid positions flanking the protein domains and constructs. The region between the SH3 and the GUK domain shows homology to HOOK domains. (B) MCF7 cells were treated for 72 h with siRNA duplexes specific for hDlg1 (middle panels) or MPP7 (bottom panels). Cells were stained with hDlg1 and MPP7 antibodies as indicated. Both antibodies showed plasma membrane staining in control-siRNA treated cells (Ctrl-siRNA, top panels). (C) Immunoblots demonstrating selective depletion of the MAGUK proteins hDlg1, MPP7, and CASK. Extracts from MCF7 cells containing the indicated siRNA duplexes were probed with the antibodies indicated. Antibodies to tubulin were as loading control. (D) Results of siRNA experiments. After depletion by siRNA of hDlg1, MPP7, or CASK, plasma membrane localization was tested for the proteins listed. X, expected elimination of siRNA target; +, persistent plasma membrane localization; −, loss of plasma membrane localization; n.d., not determined. All experiments shown in Figure 3 are representatives of three independent experiments.

Gel filtration chromatography was carried out on a Superose-6 column by FPLC (Pharmacia Biotech, Newcastle upon Tyne, UK). The column was calibrated with standards of known Stokes radii as indicated in Figure 1. Two milligrams of MCF7 cell extracts were chromatographed over the column in lysis buffer (25 mM HEPES, pH 7.4, 150 mM NaCl, 1 mM $MgCl_2$, 1 mM EGTA, 5 mM NaF, 20 mM β-glycerophosphate, 100 μM Na_3VO_4, 1 mM PMSF, 1 mM benzamidine, 1 μg/ml aprotinin, and 1 μg/ml leupeptin). Equal volumes of each fraction were analyzed by SDS-PAGE and immunoblotting.

RESULTS

To elucidate the function of cell polarity proteins in mammalian epithelial cells, we searched biochemically for proteins interacting with hDlg1 (human Dlg1/SAP97 (synapse-associated protein 97, Figure 1A). hDlg1 protein-containing complexes were immuno-affinity-purified from MCF7 breast epithelial tumor cell extracts using a specific antibody (Supplementary Figure S1A in the Supplementary Data) and fractionated by gel electrophoresis. Two coprecipitating proteins of 110 and 65 kDa were visible on gels, in addition to a triplet of bands at the size expected for hDlg1 splice variants (Figure 1B, lane 1). Mass spectrometric analyses confirmed the identity of the ~140-kDa bands as hDlg1 splice variants and revealed that the other two proteins were CASK and MPP7, respectively (Figure 1B, lane 1, and Supplementary Figure S2). CASK and MPP7 were not present when immunoprecipitation was performed with a control antibody (Figure 1B, lane 2). The identity of these proteins was confirmed by coimmunoprecipitation and Western blot analysis with specific antibodies (Figure 1C, lane 1, and Supplementary Figure S1A).

hDlg1, CASK, and MPP7 are all members of the MAGUK family of proteins, the defining features of which are at least one PDZ domain, followed by an SH3 domain and a catalytically inactive guanylate kinase domain (Funke *et al.*, 2005). CASK contains an additional amino-terminal region homologous to calcium/calmodulin-dependent protein kinase II and has previously been shown to interact with

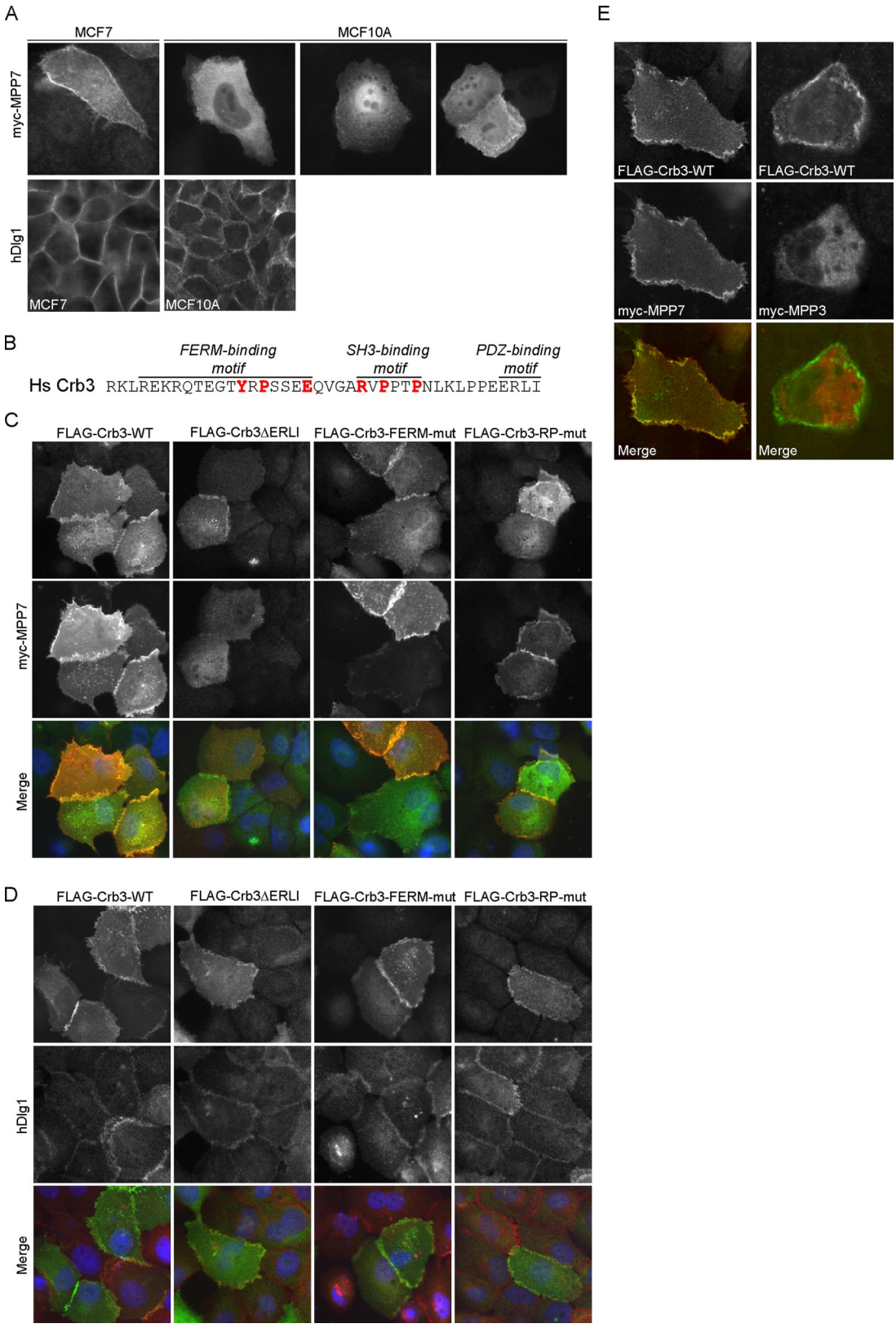

Figure 4. Crb3 recruits MPP7 to the plasma membrane. (A) MCF7 and MCF10A cells were transfected with myc-MPP7, fixed 48 h after transfection, and stained with anti-myc antibodies (top panels). Note the absence of plasma membrane staining in MCF10A cells. MCF7 and MCF10A cells were fixed and stained with antibodies for endogenous hDlg1 (bottom two panels). (B) Amino acid sequence of intracellular region of Crb3. The FERM-, SH3-, and PDZ-binding motifs are shown with lines. Alanine substitutions in key residues of these motifs to create Crb3 mutants are highlighted in red. (C) MCF10A cells were transiently cotransfected with myc-MPP7 and either FLAG-Crb3-WT, FLAG-Crb3ΔERLI (deletion of the four C-terminal residues), FLAG-Crb3-FERM-mut (point mutations in the FERM binding motif) or

hDlg1 (Nix *et al.*, 2000; Lee *et al.*, 2002). MPP7 is a so far uncharacterized member of the p55 subfamily of MAGUKs (Funke *et al.*, 2005). Importantly, we could recover both proteins associated with hDlg1 in immunoprecipitates from a wide range of epithelial cell lines derived from different tissues (Figure 1C, lanes 2–6) independently of whether the cells were polarized or not (data not shown).

To characterize further the hDlg1 complexes, we first examined whether the interaction between hDlg1, MPP7, and CASK represented one or more distinct complexes. Size exclusion chromatographic fractionation of MCF7 lysates followed by Western blotting revealed that cellular hDlg1 elutes at a size of ~500–600 kDa, suggesting one or more multimolecular complexes (Figure 1D, top). A fraction of MPP7 and CASK also eluted at a similar position to hDlg1 (Figure 1D, middle and bottom), though the majority of the cellular pool of these two proteins eluted elsewhere. Several MPP7 splice variants eluted mainly at around 200 kDa, whereas the bulk of CASK eluted as a 300-kDa complex (Figure 1D, middle and bottom). The same comigration pattern of hDlg1, MPP7, and CASK was obtained using cell extracts of unpolarized (i.e., in low calcium) MCF7 cells (data not shown). Interestingly, the elution profile of CASK and MPP7 in the hDlg1 region was slightly different, suggesting the existence of two distinct hDlg1 complexes.

To examine this further, myc-tagged MPP7 or VSVG-tagged CASK were ectopically expressed in HEK 293T cells. Immunoprecipitation with an anti-myc antibody followed by Western blot analysis revealed an interaction between myc-MPP7 and endogenous hDlg1, but not between myc-MPP7 and endogenous CASK (Figure 1E, lane 3). In contrast, anti-VSVG antibodies coprecipitated VSVG-CASK and endogenous hDlg1, but not endogenous MPP7 (Figure 1E, lane 8). Moreover, in the presence of myc-MPP7, the amount of endogenous CASK associated with endogenous hDlg1 was reduced, whereas in the presence of VSVG-CASK significantly less endogenous MPP7 could be detected in an hDlg1 immunoprecipitate (Figure 1E, lanes 2, 7, and 11). We conclude that CASK and MPP7 compete for the same or overlapping binding sites on hDlg1.

A previous report demonstrated that the interaction between hDlg1 and CASK is mediated through L27 domains present on both proteins (Lee *et al.*, 2002). To map the interaction sites of MPP7 with hDlg1, myc-tagged MPP7 deletion constructs were expressed in HEK 293T cells, and anti-myc immunoprecipitations probed on Western blots for endogenous hDlg1. Full-length myc-MPP7 could readily be coprecipitated with endogenous hDlg1 and vice versa (Figure 1F, lane 1, and data not shown); however, removal of the L27N domain of MPP7 abolished the interaction (Figure 1F, lane 2), indicating that this protein motif is required for binding to hDlg1. In agreement with this, a fragment comprising the L27N and L27C domains only of MPP7 was sufficient to specifically associate with endogenous hDlg1 (Figure 1F, lane 8). These results point to an interaction between the L27 domain of hDlg1 and the L27 domains of MPP7. To test this, key hydrophobic residues were substituted with a polar hydrophilic residue within the L27N (L38S) or L27C (L95S) domains of MPP7. myc-MPP7 and myc-MPP7/L95S coprecipitated with endogenous hDlg1 when expressed in HEK 293T cells using either myc or hDlg1 antibodies (Figure 1G, lanes 1 and 3), whereas myc-MPP7/L38S did not (Figure 1G, lane 2). We conclude that hDlg1 exists in two discrete complexes with either MPP7 or CASK in epithelial cells and that both proteins use L27 domains to interact with hDlg1.

Because hDlg1 forms two separate protein complexes with MPP7 and CASK, we made use of Caco-2 cells to examine their subcellular localization. Unlike MCF7 cells, Caco-2 cells are capable of establishing a highly polarized morphology in tissue culture conditions. We raised an antibody to MPP7 for immunofluorescence studies and found that endogenous MPP7 associates primarily with lateral membranes and is largely excluded from the basal site in polarized Caco-2 cells (Figure 2, A and B). hDlg1 is both lateral and basal and therefore colocalizes with MPP7 along the lateral side (Figure 2A). In contrast, the basolateral protein CASK only partially overlaps with MPP7 at the lateral site (Figure 2B), but colocalizes with hDlg1 along the basal membrane (data not shown, Lee *et al.*, 2002). Interestingly, MPP7 is found slightly more apical along the lateral membrane than hDlg1 (Figure 2A, right panel, inset, arrowhead). In addition, both MPP7 and hDlg1 overlap with markers for adherens junctions (Figure 2, C and D) and tight junctions (Figure 2, E and F). MPP7 staining is specific, because almost no signal is detectable in MPP7 siRNA treated cells (Supplementary Figure S1, B and C).

To examine the potential interdependency for plasma membrane localization of MPP7 and hDlg1, we returned to a more easily transfectable epithelial cell line, MCF7. First, it has previously been reported that the association of hDlg1 with the plasma membrane is dependent on the cortical actin cytoskeleton (Reuver and Garner, 1998). Treatment of MCF7 cells with cytochalasin D for 1 h to disassemble the actin cytoskeleton induced a cytoplasmic relocalization of both endogenous hDlg1 and MPP7 (Figure 2G). Next, a series of myc-tagged MPP7 deletion constructs were introduced into MCF7 cells and analyzed by immunofluorescence microscopy with anti-myc antibodies (Figures 3A and Supplementary Figure S3). Full-length myc-MPP7 localized to the plasma membrane similarly to endogenous protein. However, deletion of the amino-terminal, hDlg1-interacting L27N domain abolished membrane localization of MPP7 (Figures 3A and Supplementary Figure S3). Surprisingly, further analysis of deletion constructs revealed a second domain required for membrane localization of MPP7. A mutant lacking the SH3-HOOK domain also did not localize to the plasma membrane despite containing the L27N domain (Figures 3A and Supplementary Figure S3). We conclude that both the hDlg1-interacting L27N domain and the SH3-HOOK regions are required for targeting of MPP7 to the plasma membrane.

To examine whether the interaction with hDlg1 is required for membrane localization, gene silencing by siRNA was used in MCF7 cells. Immunofluorescence microscopy and immunoblotting demonstrated efficient and uniform hDlg1 depletion (Figure 3, B and C). In the absence of hDlg1, endogenous MPP7 no longer localizes to the plasma membrane (Figure 3B, middle

Figure 4 (cont). FLAG-Crb3-RP-mut (point mutations in the RxPPxP motif) as indicated. Cells were fixed 36 h after transfection and stained with mouse monoclonal anti-myc (red) and rabbit polyclonal anti-FLAG (green) antibodies. (D) MCF10A cells were transiently transfected with FLAG-tagged Crb3 constructs as described in C. Cells were fixed 36 h after transfection and stained with mouse monoclonal anti-hDlg1 (red) and rabbit polyclonal anti-FLAG (green) antibodies. (E) MCF10A cells were transiently cotransfected with myc-MPP7 and FLAG-Crb3-WT (first column) or myc-MPP3 and FLAG-Crb3-WT (second column) as indicated. Cells were fixed 36 h after transfection and stained with mouse monoclonal anti-myc (red) and rabbit polyclonal anti-FLAG (green) antibodies. All experiments shown in Figure 4 are representatives of three independent experiments.

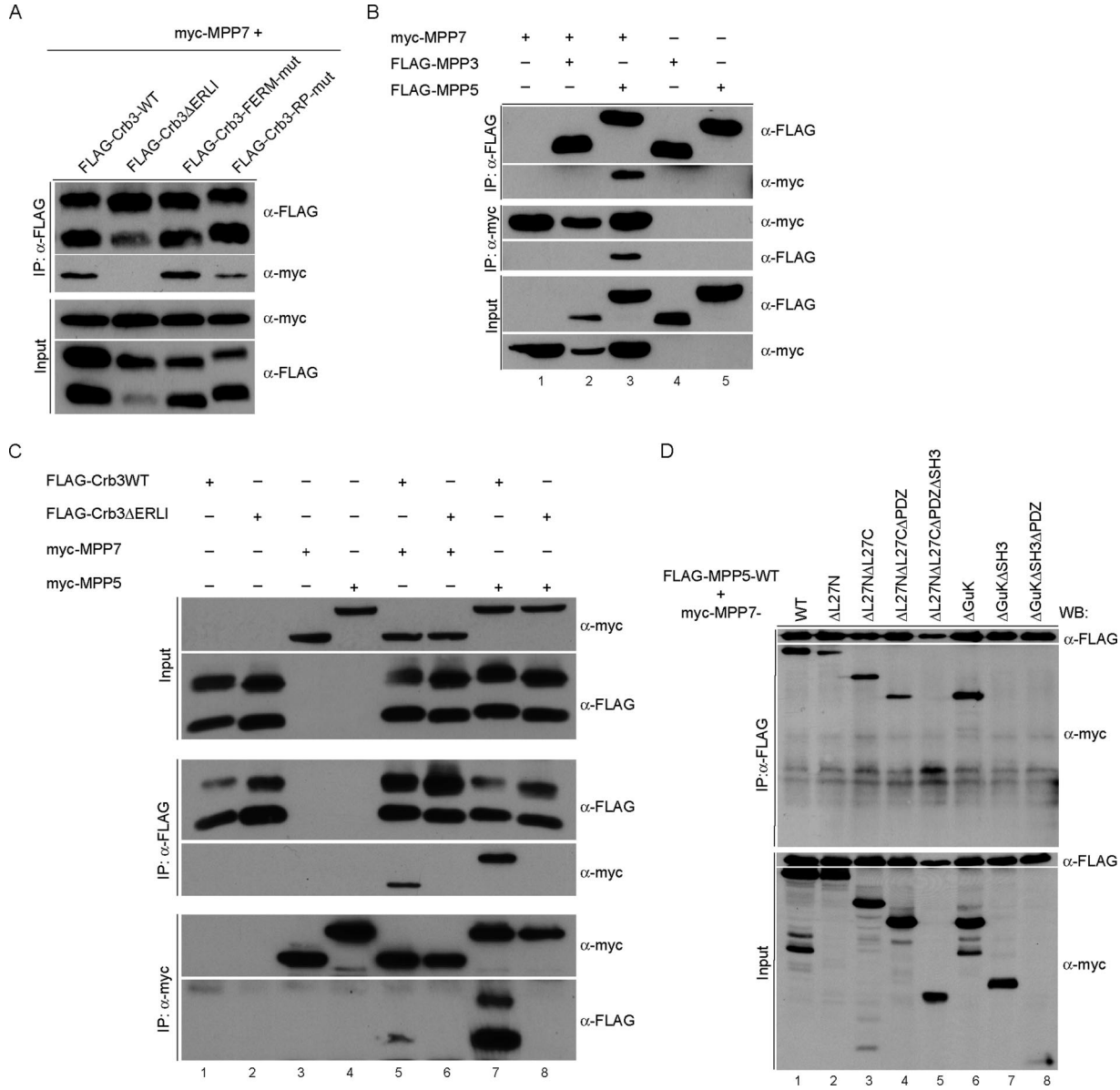

Figure 5. MPP7 binding to Crb3 is indirectly mediated via PALS1 (MPP5). (A) Immunoprecipitations were performed using FLAG antibodies from HEK 293T cells cotransfected with myc-MPP7 and FLAG-tagged Crb3 constructs as indicated. Samples of the lysates and FLAG IPs were analyzed by Western Blotting for myc and the FLAG epitope. (B) HEK 293T cells cotransfected with myc-MPP7 and FLAG-MPP5 or FLAG-MPP3, respectively, were lysed, proteins were immunoprecipitated with either myc or FLAG antibodies and proteins then visualized by immunoblot analysis with FLAG or myc antibodies as indicated. (C) Immunoprecipitations were performed using FLAG or myc antibodies from HEK 293T cells cotransfected with FLAG-Crb3-WT (lanes 1, 5, and 7), FLAG-Crb3-ΔERLI (lanes 2, 6, and 8), myc-MPP7 (lanes 3, 5, and 6), and myc-MPP5 (lanes 4, 7, and 8) as indicated. Samples of the lysates (Input) and myc- and FLAG IPs were analyzed by Western blotting for the myc and FLAG epitope. (D) Immunoprecipitations were performed using either FLAG or myc antibodies from HEK 293T cells cotransfected with FLAG-MPP5-WT and myc-tagged MPP7 constructs as indicated in the figure. Expression of the transfected constructs was monitored by Western blotting with anti-myc or anti-FLAG antibodies (Input). All experiments shown in Figure 5 are representatives of three independent experiments.

row), although strong membrane staining can be seen in control cells and in untransfected cells (Figure 3B, top row). Components of adherens junctions, such as E-cadherin, and tight junction markers, such as occludin, appeared to localize normally at the plasma membrane in the absence of hDlg1 (Figure 3D; data not shown). In contrast, depletion of MPP7 by siRNA did not interfere with the membrane localization of hDlg1 (Figure 3B, bottom). Thus, the recruitment of MPP7 to the plasma membrane is dependent on hDlg1.

Our observation that the SH3-HOOK domain in MPP7 functions as an additional membrane-targeting domain prompted us to investigate the underlying mechanism. We hypothesized that proteins other than hDlg1 might function through the SH3-HOOK domain. In fact, although myc-MPP7 similarly localized to the plasma membrane of several cell types, we noticed that it did not localize to the membrane when expressed in MCF10A mammary breast epithelial cells, despite high level expression and normal plasma

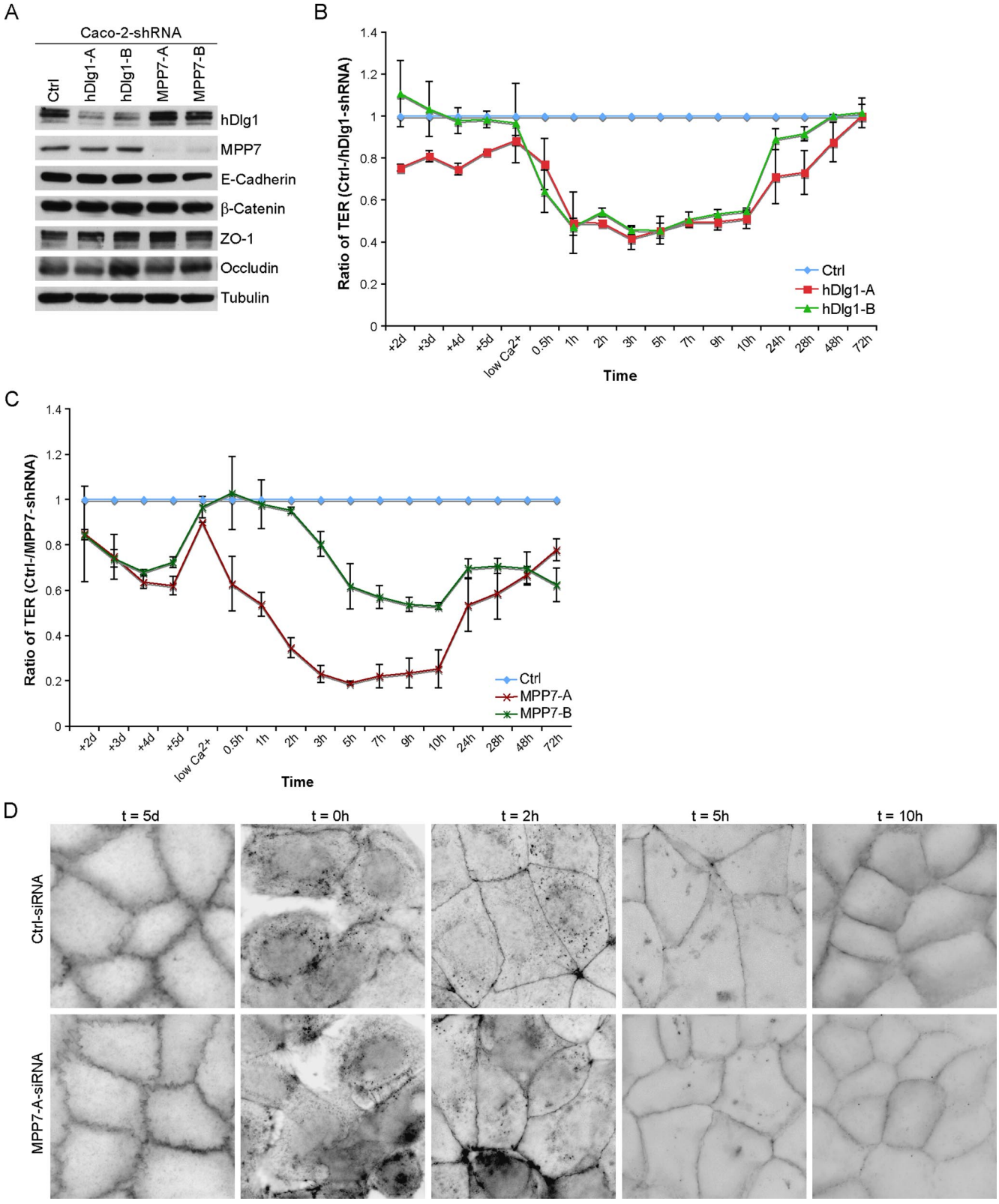

Figure 6. hDlg1 and MPP7 are necessary for tight junction integrity. (A) Lysates from Caco-2 control-shRNA and two independent hDlg1-shRNA (hDlg1-A and -B) and two independent MPP7-shRNA (MPP7-A and -B) expressing pools of cells were analyzed by Western blotting with antibodies against hDlg1 and MPP7. Immunoblots demonstrating the selective depletion of the MAGUK proteins hDlg1 and MPP7, but not of cell junction components. Antibodies to tubulin were used to demonstrate equal loading. Note the different suppression levels in MPP7-A– and MPP7-B-shRNA–expressing cell lines. (B) Transepithelial electrical resistance (TER) measurements of Caco-2 cells stably expressing Ctrl-, hDlg1-A-, and hDlg1-B-shRNA as indicated. Caco-2 cell lines were seeded onto Transwell filters and grown at confluence for 5 d. After incubation in low-calcium medium for 16 h, the cells were incubated in normal growth medium, and the restoration

membrane localization of endogenous hDlg1 in these cells (Figure 4A). A recent report showed that MCF10A fail to form tight junctions, because they express very low levels of the apical polarity transmembrane determinant, Crb3 (Fogg *et al.*, 2005). To examine whether Crb3 might also affect MPP7 localization, FLAG-tagged Crb3 together with myc-MPP7 were cotransfected into MCF10A cells and analyzed by immunofluorescence microscopy. In Crb3-expressing cells, myc-MPP7 was recruited to the plasma membrane (Figure 4C, first column), whereas it remained cytosolic when expressed with a Crb3 construct lacking the C-terminal PDZ-binding motif (Figure 4, B and C, second column). Importantly, the localization of endogenous hDlg1 remained unaffected in MCF10A cells expressing FLAG-Crb3-ΔERLI, illustrating a requirement of Crb3 in plasma membrane localization of MPP7 (Figure 4D). myc-MPP3, the closest homolog of MPP7 in the p55 MAGUK family, was not recruited to the plasma membrane in a Crb3-dependent manner in MCF10A cells, demonstrating a specific effect of Crb3 on MPP7 (Figure 4E, compare first and second columns). As shown previously, both the L27N and the SH3-HOOK domains are required for membrane targeting of MPP7 (Figure 3A, second column). In agreement, transfection of deletion constructs of MPP7 (Figure 3A, third column) with full-length Crb3 revealed that indeed the SH3-HOOK domain of MPP7 is required for Crb3-mediated membrane targeting (data not shown). In summary, these data suggest that plasma membrane localization of MPP7 is dependent on its L27N domain-mediated binding with hDlg1 and on a Crb3-dependent recruitment via the SH3-HOOK domain.

To provide further evidence for an interaction between MPP7 and Crb3, HEK 293T cells were transfected with myc-tagged MPP7 and FLAG-tagged wild-type and mutant forms of Crb3. Myc-MPP7 was not detected in immune precipitates with the PDZ-binding-site mutant of Crb3, whereas it readily coprecipitated with the wild-type, the FERM-, and the RP-motif mutants (Figure 5A). Previous studies have shown that the PDZ-binding motif of Crb3 binds to PALS1/MPP5, another member of the p55 subfamily of MAGUK proteins (Bachmann *et al.*, 2001; Hong *et al.*, 2001; Roh *et al.*, 2002b, 2003). To examine whether the interaction between MPP7 and Crb3 is directly or indirectly mediated by PALS1 (MPP5), wild-type and deletion constructs of MPP7 were examined for their ability to interact with MPP5. HEK 293T cells were cotransfected with myc-tagged MPP7 and FLAG-tagged MPP5, and, as shown in Figure 5B (lane 3), myc-MPP7 can be coprecipitated with FLAG-MPP5 and vice versa. Importantly, MPP3, another member of the p55 subfamily of MAGUKs, did not interact with myc-MPP7, suggesting a specific interaction between MPP7 and PALS1 (MPP5; Figure 5B, lane 2). Moreover, PALS1 (MPP5) associated much more efficiently with Crb3 than MPP7 (Figure 5C, compare lanes 5 and 7), supporting the idea that MPP7 binding to Crb3 is indirectly mediated via its interaction with PALS1 (MPP5). Importantly, the interaction with PALS1 (MPP5) required the SH3-HOOK domain, but not the PDZ domain of MPP7 (Figures 3A, fourth column, and 5D, compare lanes 4, 6, and 7), excluding a potential unspecific interaction with the PDZ-binding motif of Crb3.

Because hDlg1 and MPP7 show overlapping localization to tight junctions, we directly investigated whether these proteins are required for the functional assembly of epithelial tight junctions. To examine this, pools of Caco-2 cells stably depleted of either hDlg1 or MPP7 by infection with retroviral-mediated shRNA were established. Western blot analysis confirmed that protein expression of the two proteins was attenuated (Figure 6A). To assess tight junction function, we measured transepithelial electrical resistance (TER) as a quantitative readout for tight junction integrity in combination with a calcium-switch assay. hDlg1 and MPP7-depleted Caco-2 cells were plated on collagen-coated filters and grown to confluence over 5 d to establish polarity. The medium was then replaced with a low-calcium medium, and the cells were left overnight to disrupt cell–cell contacts. After this time, normal growth medium was readded and TER was measured over a 3-d time course. Control cells rapidly reformed tight junctions within 10–15 h after returning to normal growth medium (Supplementary Figure S4, A and B), whereas there was a delay in the formation of tight junctions in the hDlg1-depleted cell lines (Figures 6B and Supplementary Figure S4A). shRNA-mediated elimination of MPP7 led to a significant retardation of the development of TER and the extent of TER inhibition correlated with the degree of MPP7 suppression (Figure 6, A and C, and Supplementary Figure S4B). Moreover, the start and end point TER-values remained significantly lower than of control cells, suggesting that MPP7 may also be involved in tight junction maintenance. To examine whether the defects observed in Caco-2 cells lacking hDlg1 or MPP7 correlated with improper localization of cell junction proteins, cells were fixed and stained after the calcium-switch assays. In low-calcium medium, cell–cell junctions were completely disrupted as shown in Figure 6D (t = 0 h). However, we found no obvious mislocalization of tight junction markers, such as occludin and ZO-1 (Figure 6D and data not shown), or adherens junction markers, such as E-cadherin and β-catenin (data not shown).

Figure 6 (cont). of cell junctions was monitored by measuring TER, expressed in Ω/cm^2. Results were plotted as the relative values of TER (for hDlg1-A- and hDlg1-B-shRNA) compared with the TER of Ctrl-shRNA (set TER = 1 for every time point). Values have been corrected for background and represent the mean of data taken in three independent experiments (and per experiment in duplicate). Error bars, SD between individual measurements. (C) Transepithelial electrical resistance (TER) measurements of Caco-2 cells stably expressing Ctrl-, MPP7-A- and MPP7-B-shRNA as indicated. Measurements and cell culture was performed as described in B. (D) Caco-2 cell lines were seeded onto Transwell filters and grown at confluence for 5 d. After incubation in low-calcium medium for 16 h, the cells were incubated in normal growth medium and at different times (shown for t = 0, 2, 5, and 10 h) were fixed, permeabilized, and immunostained with anti-occludin antibodies. For better visualization of cell borders and cytoplasmic aggregates of tight junction components, immunostaining is shown in the inverted mode.

DISCUSSION

In *Drosophila*, Dlg1 plays an important role in the establishment of cell polarity during epithelial morphogenesis and asymmetric cell division in neuroblasts (Macara, 2004; Wodarz, 2005). The protein is located basolaterally in polarized epithelia (Bilder and Perrimon, 2000), but its biochemical role is not at all clear. Interestingly, in migrating primary astrocytes Dlg1 localizes to the leading edge in a Par6/aPKC-dependent manner, where it interacts with the microtubule-bound adenomatous polyposis coli (APC) tumor suppressor protein to regulate microtubule cytoskeleton polarity (Etienne-Manneville *et al.*, 2005). Here we identify MPP7, a member of the p55 subfamily of MAGUK proteins, as a new binding partner of Dlg1 in human epithelial cells.

We find that the N-terminal L27 domain in MPP7 interacts with hDlg1. Through its SH3-HOOK domain, MPP7 also interacts with PALS1 (MPP5), a member of the Crb3/PALS1 (MPP5)/PATJ group of apically localized polarity proteins, and in turn PALS1 (MPP5) interacts with Crb3 (Bachmann *et al.*, 2001; Hong *et al.*, 2001; Roh *et al.*, 2002b, 2003). In Caco-2 cells, we find that both hDlg1 and MPP7 show partial colocalization with Occludin and ZO-1, suggesting that the interaction of these polarity complexes might occur at the level of cell junctions. However, it remains unclear whether all these proteins are simultaneously present in one complex.

We also provide evidence that MPP7 can interact with Crb3 likely through its interaction with MPP5 (PALS1). A recent report on the identification of new polarity complexes showed that MPP7 can be coprecipitated with PALS1 (MPP5) and PATJ (Wells *et al.*, 2006), thus validating our data. This raises the possibility that MPP7 might act as a bridge between the Dlg and Crb groups of polarity proteins. However, we have been unable to detect any Crb3 or PALS1 (MPP5) in hDlg1 immunoprecipitates (data not shown) and so this remains speculative. It is possible that the interaction between MPP7 and the Crb3/PALS1 (MPP5) complex is transient and that MPP7 is recruited to the plasma membrane through an interaction between its SH3-HOOK domain and PALS1 (MPP5) and is then retained at the cell membrane through binding to hDlg1. This would account for our observation that hDlg1 is required, but not sufficient, for the localization of MPP7 to the plasma membrane. Such a two-step mechanism for plasma membrane recruitment is already known for several polarity proteins, e.g., Dlg1 (Thomas *et al.*, 2000) and Scribble (Albertson *et al.*, 2004; Zeitler *et al.*, 2004).

Finally, we provide evidence that the interaction of hDlg1 and MPP7 is functionally important in tight junction formation. Retroviral-shRNA mediated depletion of either MPP7 or hDlg1 compromised functional tight junctions assembly in Caco-2 cells after a calcium switch, as revealed by quantitative TER. It is clear, however, that although the loss of hDlg1 or MPP7 in Caco-2 cells leads to a defect in tight junction functionality, it does not lead to significant mislocalization of tight junction markers (occludin, ZO-1), or adherens junction proteins (E-cadherin, β-catenin). A similar conclusion has been reached in hScrib-depleted cells (Qin *et al.*, 2005). This may suggest that MPP7 and the Dlg/Scrib group of polarity proteins are not required for cell junction assembly, but rather for some functional activity perhaps related to its dynamic stability. Alternatively, possible redundancy in the activities and/or protein–protein interactions associated with the numerous polarity proteins, coupled with the relatively unsophisticated nature of these 2D tissue culture assays may account for the lack of dramatic phenotypes.

ACKNOWLEDGMENTS

We are grateful to Zenta Walther (Yale) for the VSVG-CASK construct, James Staddon (EISAI Research Laboratories, London, United Kingdom) for help with gel filtration chromatography and members of the laboratory for valuable discussions. V.M.S. is supported by an European Union Marie-Curie fellowship, and A.H. is generously supported by Cancer Research UK. K.G. is a Postdoctoral Fellow of the Fund for Scientific Research, Flanders, Belgium (F.W.O. Vlaanderen). The project was supported by research grants from the Fund for Scientific Research, Flanders, Belgium (project number G.0008.03) and the GBOU-research initiative (project number 20204) of the Flanders Institute of Science and Technology (IWT) to K.G. and J.V.

REFERENCES

Albertson, R., Chabu, C., Sheehan, A., and Doe, C. Q. (2004). Scribble protein domain mapping reveals a multistep localization mechanism and domains necessary for establishing cortical polarity. J. Cell Sci. *117*, 6061–6070.

Bachmann, A., Schneider, M., Theilenberg, E., Grawe, F., and Knust, E. (2001). *Drosophila* Stardust is a partner of Crumbs in the control of epithelial cell polarity. Nature *414*, 638–643.

Bilder, D. (2004). Epithelial polarity and proliferation control: links from the *Drosophila* neoplastic tumor suppressors. Genes Dev. *18*, 1909–1925.

Bilder, D., Li, M., and Perrimon, N. (2000). Cooperative regulation of cell polarity and growth by *Drosophila* tumor suppressors. Science *289*, 113–116.

Bilder, D., and Perrimon, N. (2000). Localization of apical epithelial determinants by the basolateral PDZ protein Scribble. Nature *403*, 676–680.

Bilder, D., Schober, M., and Perrimon, N. (2003). Integrated activity of PDZ protein complexes regulates epithelial polarity. Nat. Cell Biol. *5*, 53–58.

Bossinger, O., Klebes, A., Segbert, C., Theres, C., and Knust, E. (2001). Zonula adherens formation in *Caenorhabditis elegans* requires dlg-1, the homologue of the *Drosophila* gene discs large. Dev. Biol. *230*, 29–42.

Ebnet, K., Suzuki, A., Horikoshi, Y., Hirose, T., Meyer Zu Brickwedde, M. K., Ohno, S., and Vestweber, D. (2001). The cell polarity protein ASIP/PAR-3 directly associates with junctional adhesion molecule (JAM). EMBO J. *20*, 3738–3748.

Etienne-Manneville, S., Manneville, J. B., Nicholls, S., Ferenczi, M. A., and Hall, A. (2005). Cdc42 and Par6-PKCzeta regulate the spatially localized association of Dlg1 and APC to control cell polarization. J. Cell Biol. *170*, 895–901.

Fogg, V. C., Liu, C. J., and Margolis, B. (2005). Multiple regions of Crumbs3 are required for tight junction formation in MCF10A cells. J. Cell Sci. *118*, 2859–2869.

Funke, L., Dakoji, S., and Bredt, D. S. (2005). Membrane-associated guanylate kinases regulate adhesion and plasticity at cell junctions. Annu. Rev. Biochem. *74*, 219–245.

Gevaert, K., and Vandekerckhove, J. (2005). In-gel digestion of protein spots for mass spectrometry. In: Cell Biology Handbook: A Laboratory Manual, Vol. 4, 3rd ed., ed. J. Celis, San Diego: Academic Press, Chapter 48, 379–382.

Hong, Y., Stronach, B., Perrimon, N., Jan, L. Y., and Jan, Y. N. (2001). *Drosophila* Stardust interacts with Crumbs to control polarity of epithelia but not neuroblasts. Nature *414*, 634–638.

Izumi, Y., Hirose, T., Tamai, Y., Hirai, S., Nagashima, Y., Fujimoto, T., Tabuse, Y., Kemphues, K. J., and Ohno, S. (1998). An atypical PKC directly associates and colocalizes at the epithelial tight junction with ASIP, a mammalian homologue of *Caenorhabditis elegans* polarity protein PAR-3. J. Cell Biol. *143*, 95–106.

Joberty, G., Petersen, C., Gao, L., and Macara, I. G. (2000). The cell-polarity protein Par6 links Par3 and atypical protein kinase C to Cdc42. Nat. Cell Biol. *2*, 531–539.

Lee, S., Fan, S., Makarova, O., Straight, S., and Margolis, B. (2002). A novel and conserved protein-protein interaction domain of mammalian Lin-2/CASK binds and recruits SAP97 to the lateral surface of epithelia. Mol. Cell. Biol. *22*, 1778–1791.

Lemmers, C., Medina, E., Delgrossi, M. H., Michel, D., Arsanto, J. P., and Le Bivic, A. (2002). hINADl/PATJ, a homolog of discs lost, interacts with crumbs and localizes to tight junctions in human epithelial cells. J. Biol. Chem. *277*, 25408–25415.

Lin, D., Edwards, A. S., Fawcett, J. P., Mbamalu, G., Scott, J. D., and Pawson, T. (2000). A mammalian PAR-3-PAR-6 complex implicated in Cdc42/Rac1 and aPKC signalling and cell polarity. Nat. Cell Biol. *2*, 540–547.

Macara, I. G. (2004). Parsing the polarity code. Nat. Rev. Mol. Cell Biol. *5*, 220–231.

Makarova, O., Roh, M. H., Liu, C. J., Laurinec, S., and Margolis, B. (2003). Mammalian Crumbs3 is a small transmembrane protein linked to protein associated with Lin-7 (Pals1). Gene *302*, 21–29.

Medina, E., Lemmers, C., Lane-Guermonprez, L., and Le Bivic, A. (2002). Role of the Crumbs complex in the regulation of junction formation in *Drosophila* and mammalian epithelial cells. Biol. Cell *94*, 305–313.

Nix, S. L., Chishti, A. H., Anderson, J. M., and Walther, Z. (2000). hCASK and hDlg associate in epithelia, and their src homology 3 and guanylate kinase domains participate in both intramolecular and intermolecular interactions. J. Biol. Chem. *275*, 41192–41200.

Petronczki, M., and Knoblich, J. A. (2001). DmPAR-6 directs epithelial polarity and asymmetric cell division of neuroblasts in *Drosophila*. Nat. Cell Biol. *3*, 43–49.

Qin, Y., Capaldo, C., Gumbiner, B. M., and Macara, I. G. (2005). The mammalian Scribble polarity protein regulates epithelial cell adhesion and migration through E-cadherin. J. Cell Biol. *171*, 1061–1071.

Qiu, R. G., Abo, A., and Steven Martin, G. (2000). A human homolog of the *C. elegans* polarity determinant Par-6 links Rac and Cdc42 to PKCzeta signaling and cell transformation. Curr. Biol. *10*, 697–707.

Reuver, S. M., and Garner, C. C. (1998). E-cadherin mediated cell adhesion recruits SAP97 into the cortical cytoskeleton. J. Cell Sci. *111*(Pt 8), 1071–1080.

Roh, M. H., Fan, S., Liu, C. J., and Margolis, B. (2003). The Crumbs3-Pals1 complex participates in the establishment of polarity in mammalian epithelial cells. J. Cell Sci. *116*, 2895–2906.

Roh, M. H., Liu, C. J., Laurinec, S., and Margolis, B. (2002a). The carboxyl terminus of zona occludens-3 binds and recruits a mammalian homologue of discs lost to tight junctions. J. Biol. Chem. *277*, 27501–27509.

Roh, M. H., Makarova, O., Liu, C. J., Shin, K., Lee, S., Laurinec, S., Goyal, M., Wiggins, R., and Margolis, B. (2002b). The Maguk protein, Pals1, functions as an adapter, linking mammalian homologues of Crumbs and Discs Lost. J. Cell Biol. *157*, 161–172.

Schock, F., and Perrimon, N. (2002). Molecular mechanisms of epithelial morphogenesis. Annu. Rev. Cell Dev. Biol. *18*, 463–493.

Shin, K., Straight, S., and Margolis, B. (2005). PATJ regulates tight junction formation and polarity in mammalian epithelial cells. J. Cell Biol. *168*, 705–711.

Straight, S. W., Shin, K., Fogg, V. C., Fan, S., Liu, C. J., Roh, M., and Margolis, B. (2004). Loss of PALS1 expression leads to tight junction and polarity defects. Mol. Biol. Cell *15*, 1981–1990.

Suzuki, A., Ishiyama, C., Hashiba, K., Shimizu, M., Ebnet, K., and Ohno, S. (2002). aPKC kinase activity is required for the asymmetric differentiation of the premature junctional complex during epithelial cell polarization. J. Cell Sci. *115*, 3565–3573.

Suzuki, A., Yamanaka, T., Hirose, T., Manabe, N., Mizuno, K., Shimizu, M., Akimoto, K., Izumi, Y., Ohnishi, T., and Ohno, S. (2001). Atypical protein kinase C is involved in the evolutionarily conserved par protein complex and plays a critical role in establishing epithelia-specific junctional structures. J. Cell Biol. *152*, 1183–1196.

Tabuse, Y., Izumi, Y., Piano, F., Kemphues, K. J., Miwa, J., and Ohno, S. (1998). Atypical protein kinase C cooperates with PAR-3 to establish embryonic polarity in *Caenorhabditis elegans*. Development *125*, 3607–3614.

Takekuni, K., Ikeda, W., Fujito, T., Morimoto, K., Takeuchi, M., Monden, M., and Takai, Y. (2003). Direct binding of cell polarity protein PAR-3 to cell-cell adhesion molecule nectin at neuroepithelial cells of developing mouse. J. Biol. Chem. *278*, 5497–5500.

Tanentzapf, G., and Tepass, U. (2003). Interactions between the crumbs, lethal giant larvae and bazooka pathways in epithelial polarization. Nat. Cell Biol. *5*, 46–52.

Tepass, U., Tanentzapf, G., Ward, R., and Fehon, R. (2001). Epithelial cell polarity and cell junctions in *Drosophila*. Annu. Rev. Genet. *35*, 747–784.

Thomas, U., Ebitsch, S., Gorczyca, M., Koh, Y. H., Hough, C. D., Woods, D., Gundelfinger, E. D., and Budnik, V. (2000). Synaptic targeting and localization of discs-large is a stepwise process controlled by different domains of the protein. Curr. Biol. *10*, 1108–1117.

Wells, C. D. *et al.* (2006). A. Rich1/Amot complex regulates the Cdc42 GTPase and apical-polarity proteins in epithelial cells. Cell *125*, 535–548.

Wodarz, A. (2005). Molecular control of cell polarity and asymmetric cell division in *Drosophila* neuroblasts. Curr. Opin. Cell Biol. *17*, 475–481.

Wodarz, A., Ramrath, A., Grimm, A., and Knust, E. (2000). *Drosophila* atypical protein kinase C associates with Bazooka and controls polarity of epithelia and neuroblasts. J. Cell Biol. *150*, 1361–1374.

Woods, D. F., Hough, C., Peel, D., Callaini, G., and Bryant, P. J. (1996). Dlg protein is required for junction structure, cell polarity, and proliferation control in *Drosophila* epithelia. J. Cell Biol. *134*, 1469–1482.

Yamanaka, T. *et al.* (2001). PAR-6 regulates aPKC activity in a novel way and mediates cell-cell contact-induced formation of the epithelial junctional complex. Genes Cells *6*, 721–731.

Yeaman, C., Grindstaff, K. K., and Nelson, W. J. (1999). New perspectives on mechanisms involved in generating epithelial cell polarity. Physiol. Rev. *79*, 73–98.

Zeitler, J., Hsu, C. P., Dionne, H., and Bilder, D. (2004). Domains controlling cell polarity and proliferation in the *Drosophila* tumor suppressor Scribble. J. Cell Biol. *167*, 1137–1146.